

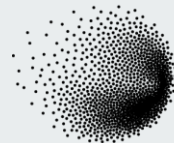


Status of the superconducting injection channels for the muEDM experiment

Pranas Juknevičius

BVR56

2025-02-10



PSI Center for Neutron and
Muon Sciences

Outline



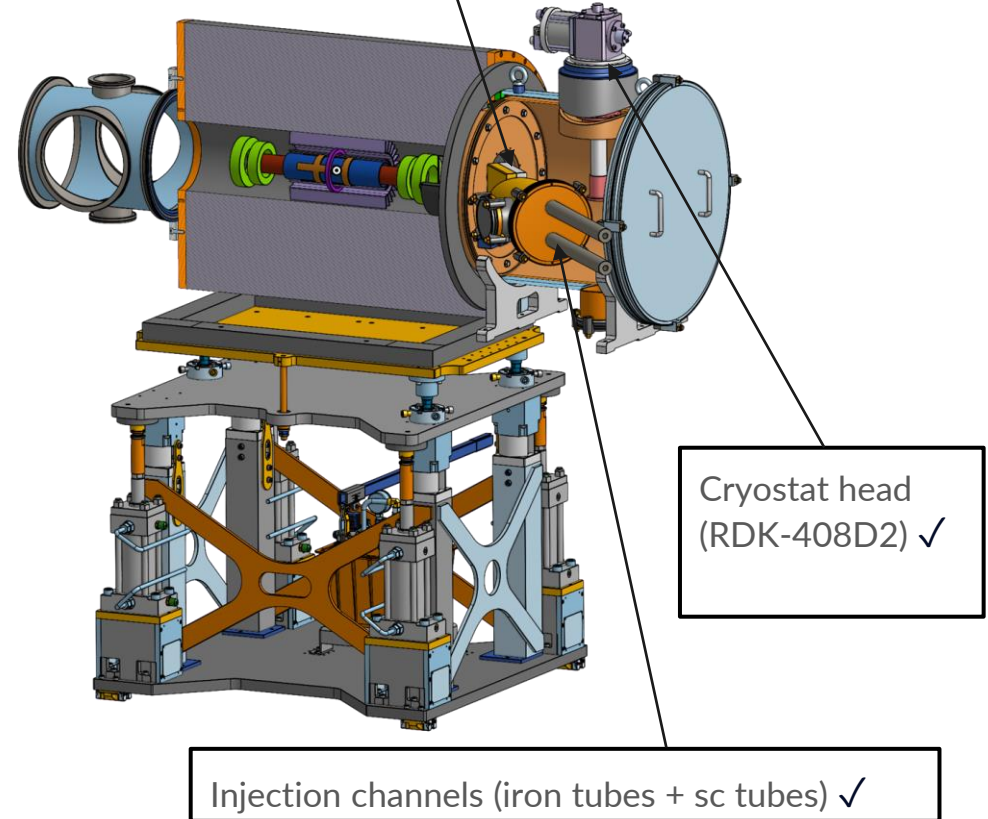
- Overview
- Thermal simulation of superconducting injection channels
- Magnetic field shielding simulation
- Magnetic field shielding and force measurement at LHe
- Conclusions

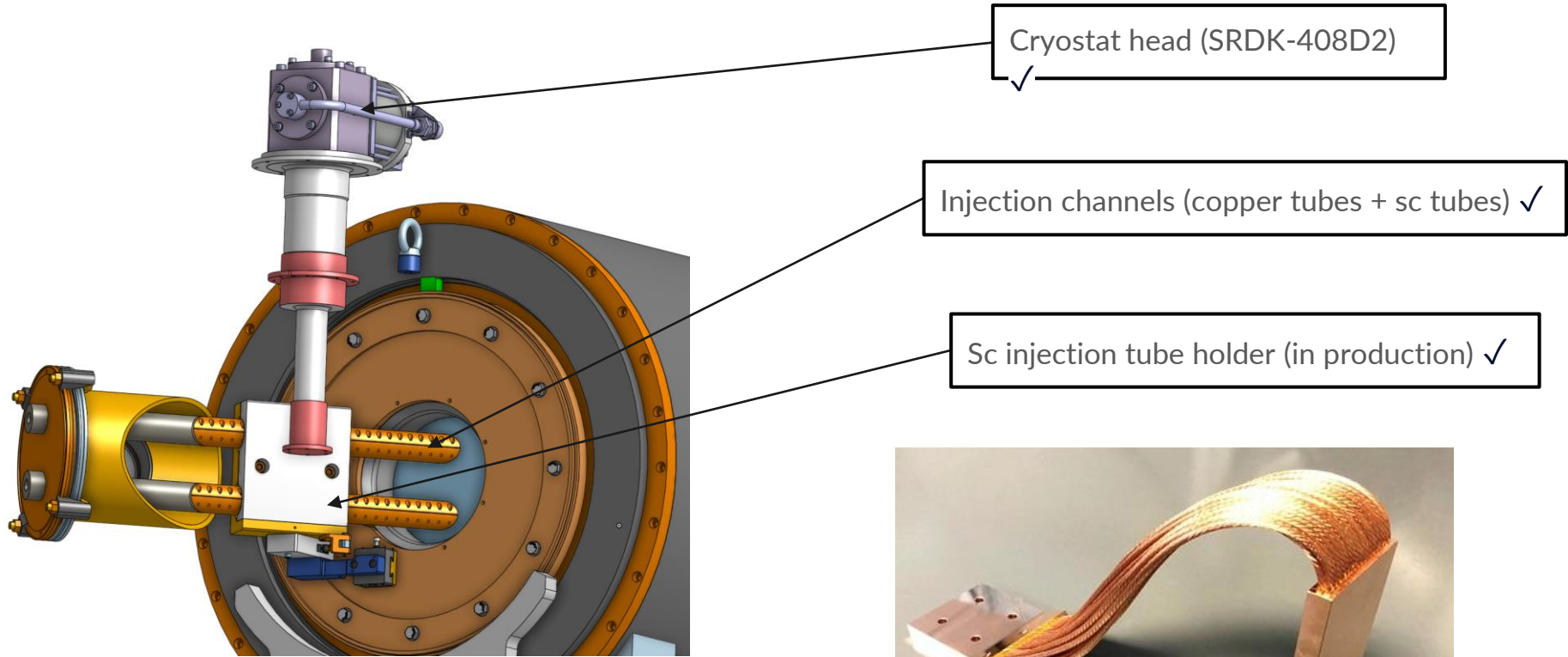
Objectives for the superconducting injection channels

Injecting muons into the bore of the 3T solenoid magnet requires penetrating the fringe field. This can be achieved by guiding the muons using superconducting hollow tubes.

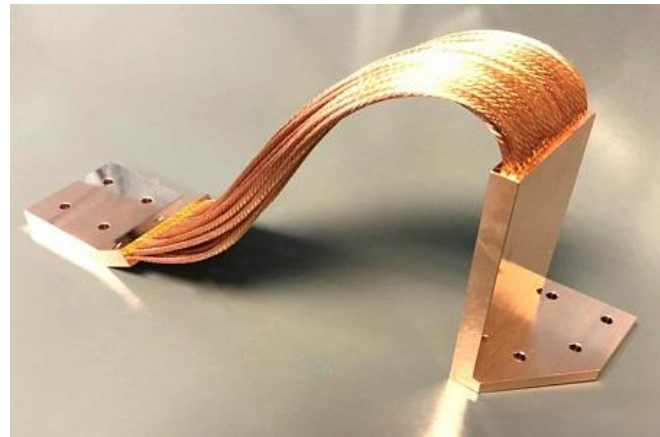
Muon storage and injection studies show that successful storage can be achieved, when inner B field transversal components < 100 mT.

Superconductors must be cooled below critical temperatures at operation.

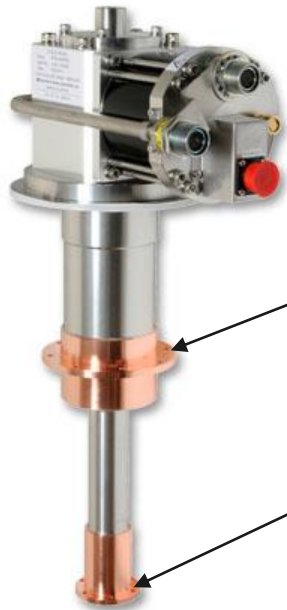




Thanks to Mike G. and Diego B. for the drawing.



SRDK-408D2 Cold head ✓



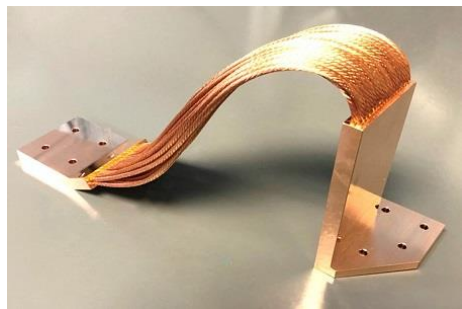
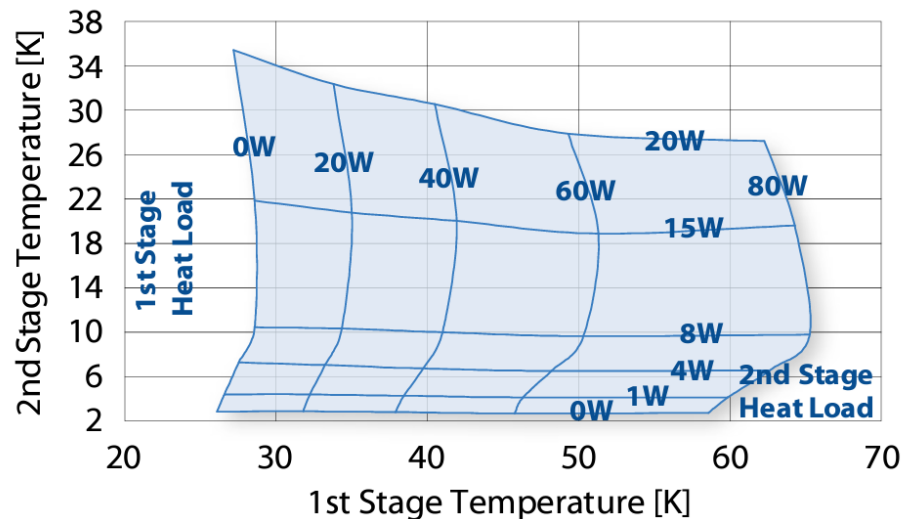
Cryostat production finishes in February

1st stage

2nd stage

SRDK-408D2 Cold Head Capacity Map (60 Hz)

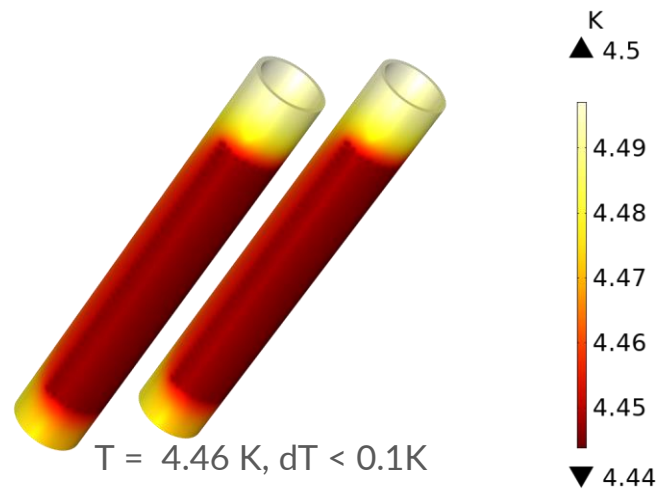
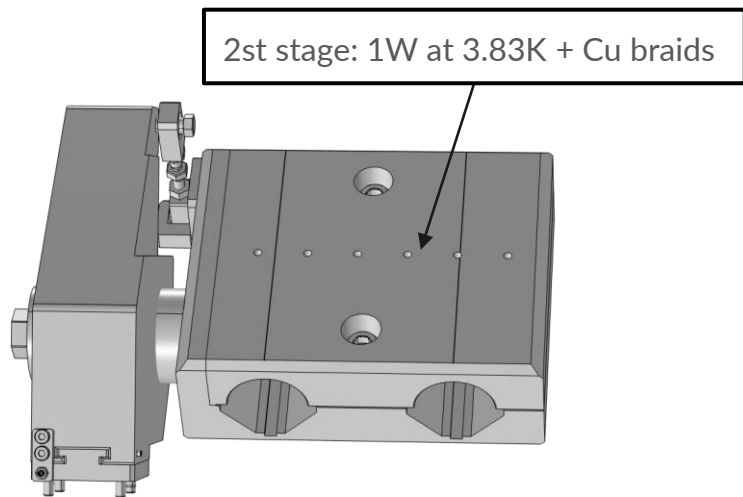
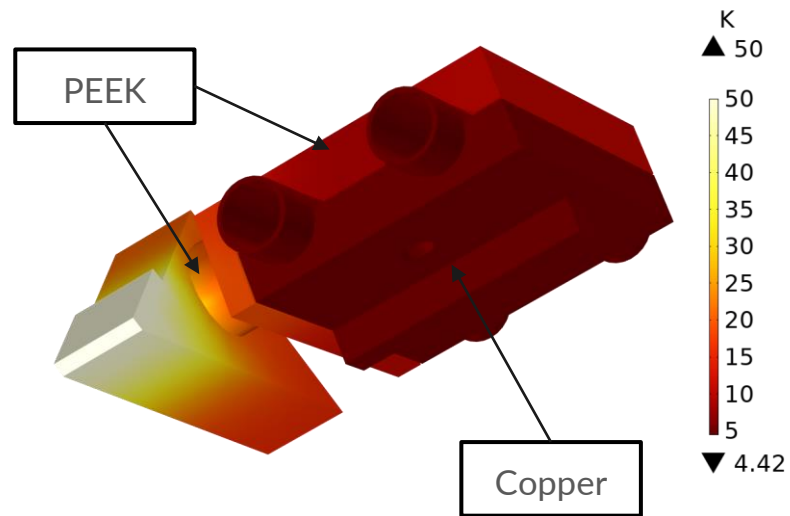
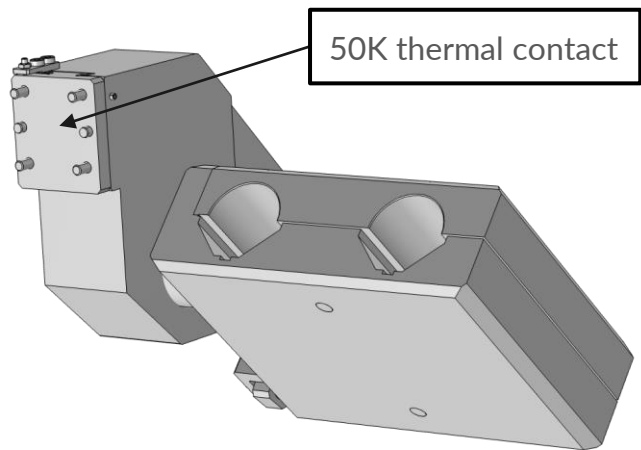
With F-50 Compressor and 6 m (20 ft.) Helium Gas Lines



Certified inspection test:

- 1st stage: 50W at 35.7K
- 2nd stage: 1W at 3.83K

Therefore we use these parameters as reference values simulation.

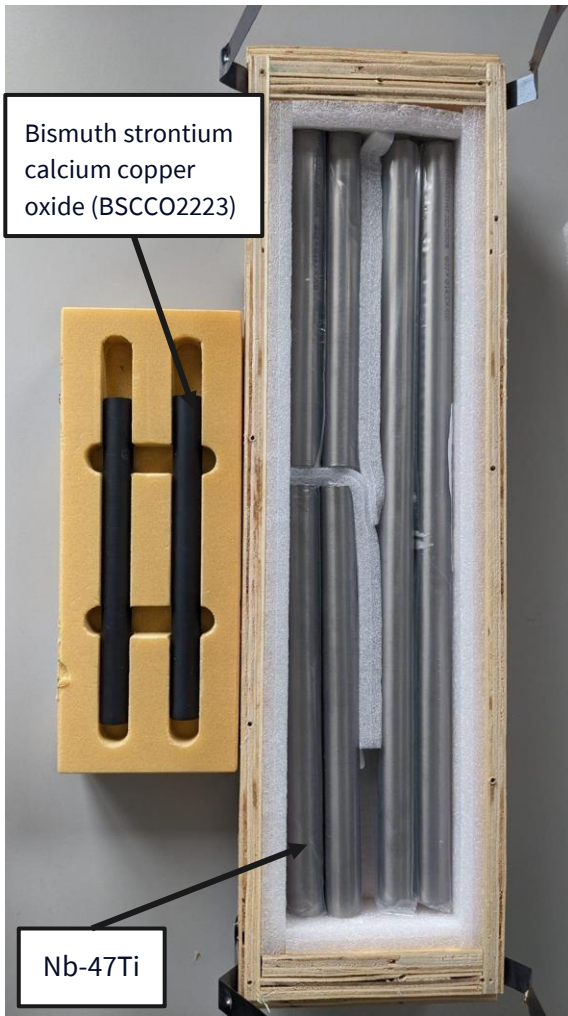


NbTi/Nb/Cu layered sheets

Used at CERN to successfully shield magnetic field up to 3.1T at 4.2K see ref:
10.1109/TASC.2018.2872860



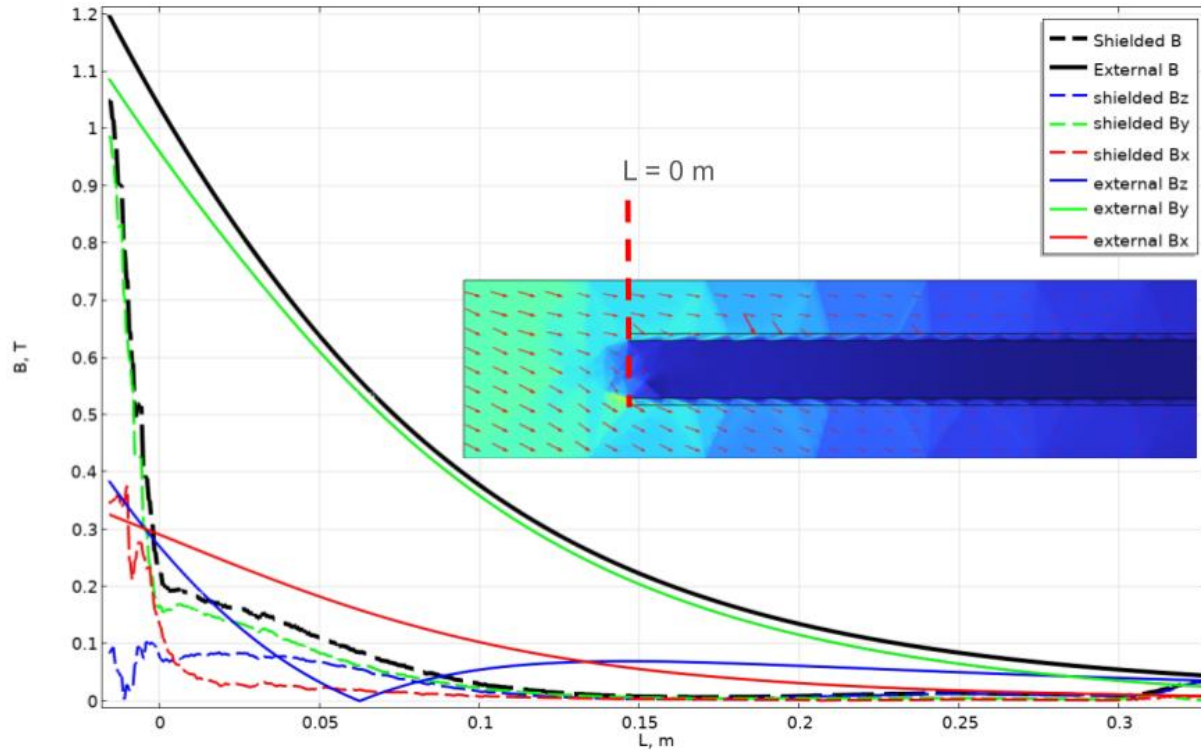
Bismuth strontium calcium copper oxide (BSCCO2223)



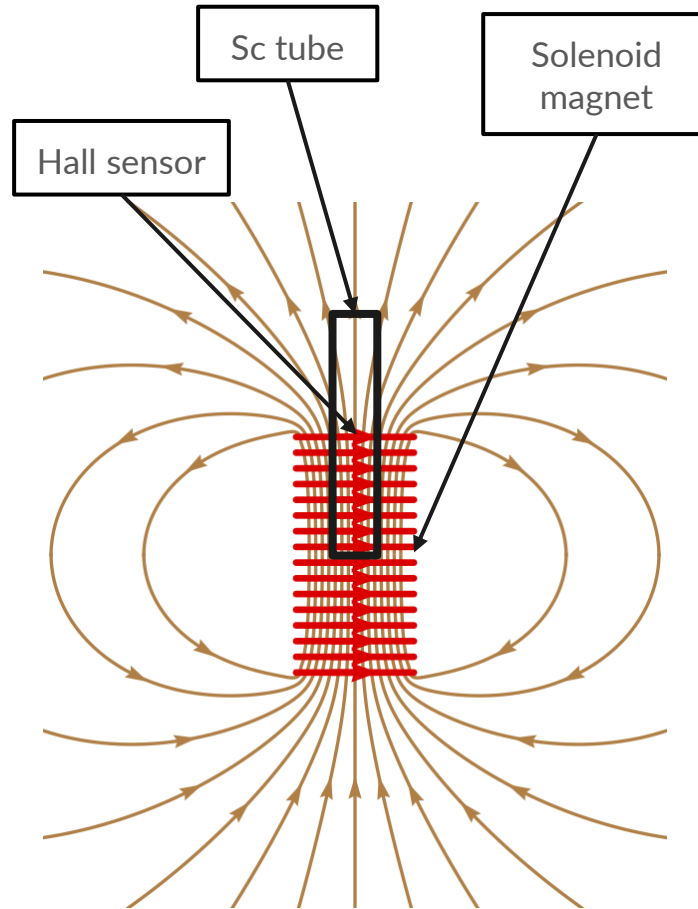
Nb-47Ti



S-Innovations 2G HTS tape 04-20Ag-5Cu-38H



Muon storage simulations show that successful storage can be achieved, when B field transversal components < 100 mT.

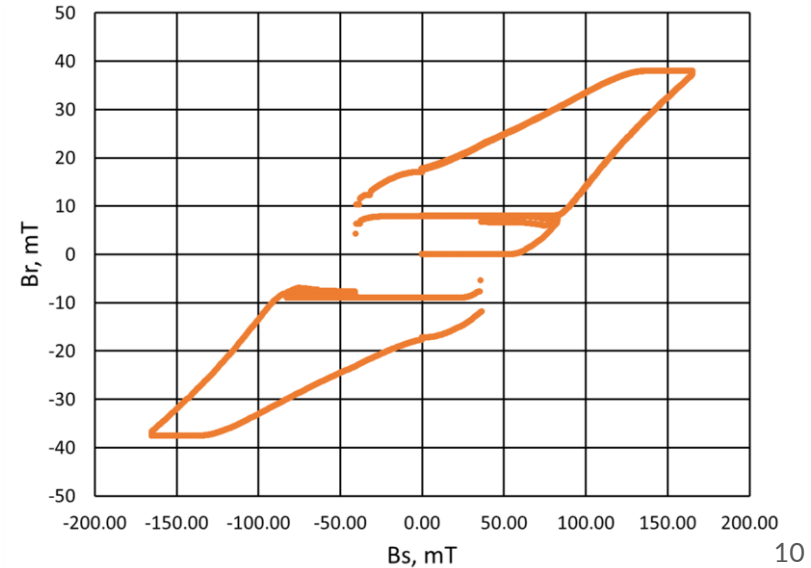
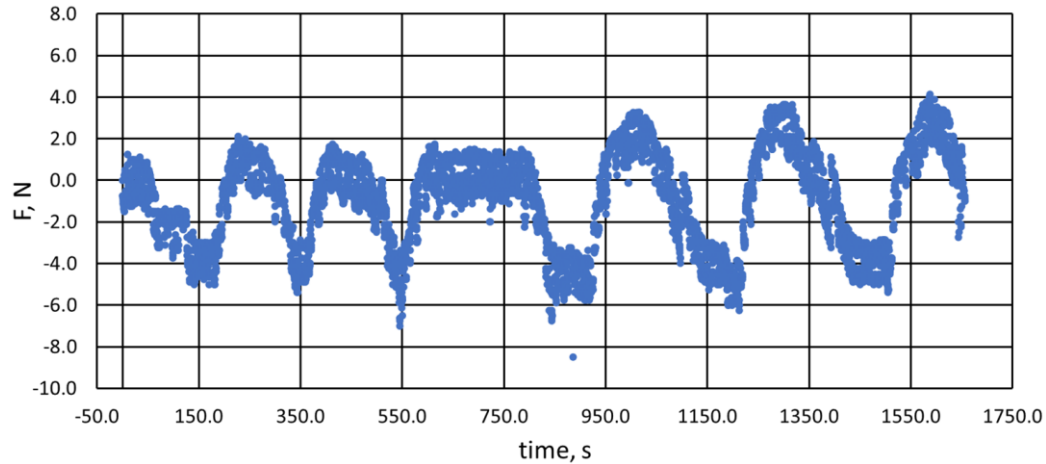
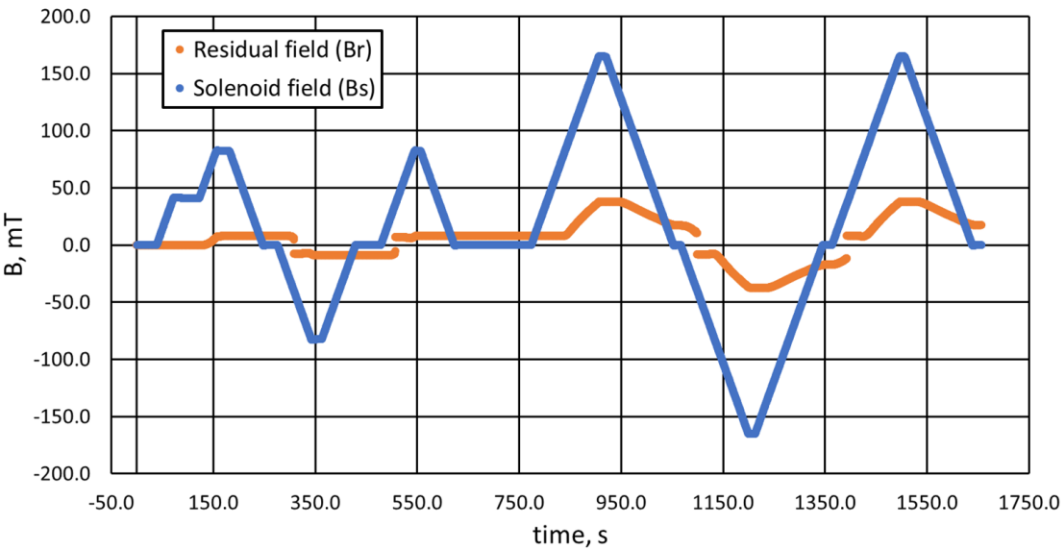


Magnetic field shielding and force measurement

- Measurements performed with **BSCCO2223** and **Nb-47Ti** superconducting tubes at LHe
- Measured **only** axial force and axial magnetic field component

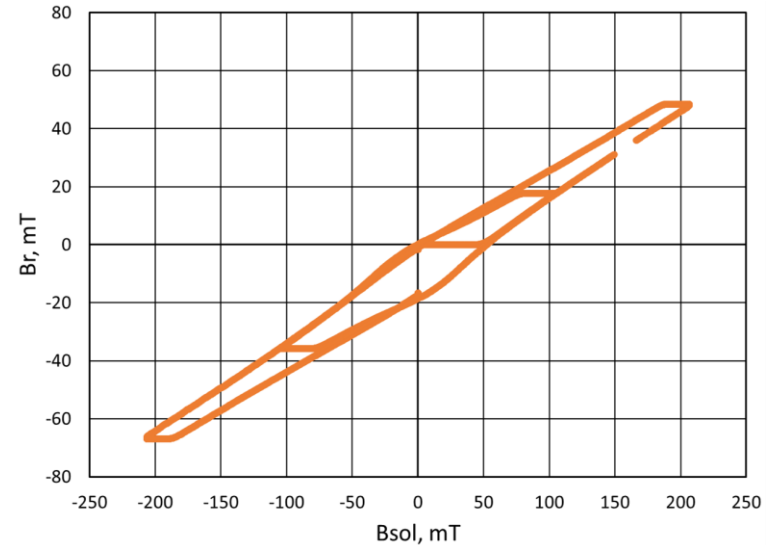
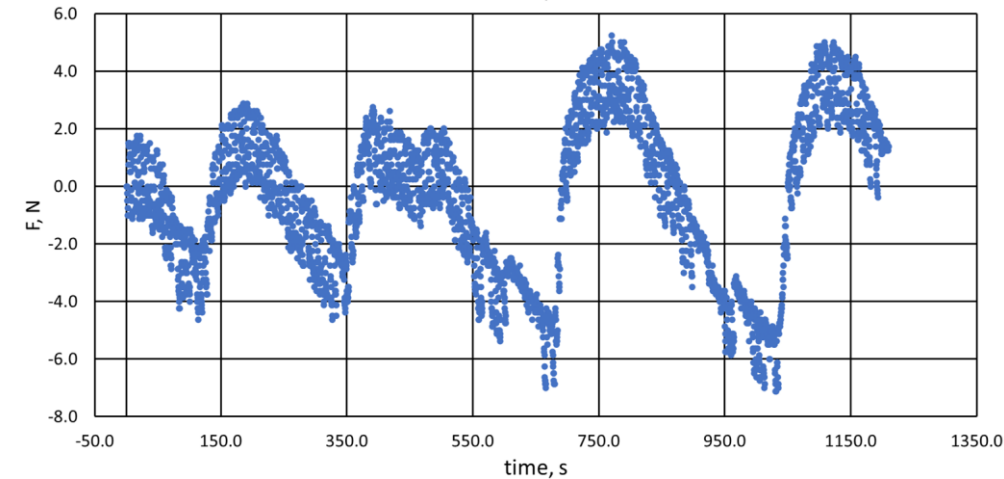
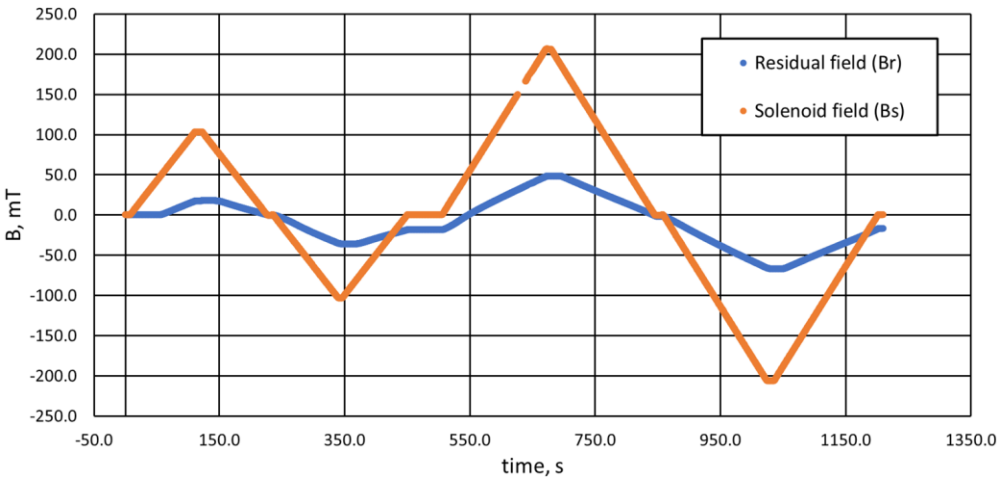
Nb-47Ti tube measurement

- Fully shielded up to 60 mT
- $SF = B_s/Br = 4.6$ at 165 mT
- $F = 5N$ @ $B_s = 165$ mT and $Br = 37$ mT (expected $F = 15N$ @ $B_s = 165mT$)



BSCCO2223 tube measurement

- Fully shielded up to 52mT at 4.2K
 - *S Denis et al 2007* reported full shielded up to 14mT at 77K
ref: 10.1088/0953-2048/20/3/014
- SF = 4.2 at 200 mT
- **F = 4N @ Bs = 200 mT and Br = 50 mT**
(expected **F = 17N @Bs = 200mT**)



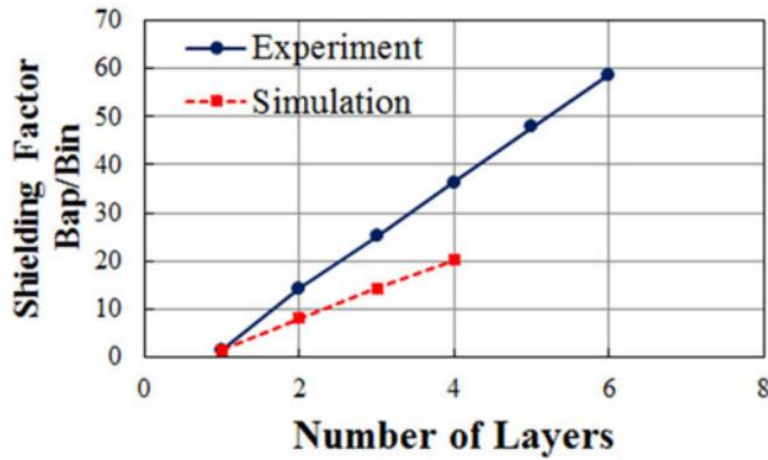


Figure taken from *Y. Nagasaki et al 2018*
 Ref: 10.1109/TASC.2018.2808374



Image taken from *Y. Nagasaki et al 2018*
 Ref: 10.1109/TASC.2018.2808374

Cylindrical shields with REBCO tapes

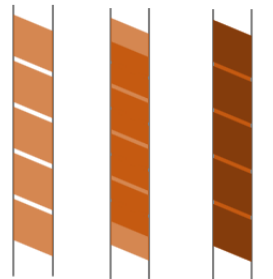
Configuration 1

Steel tube, 15 mm \varnothing



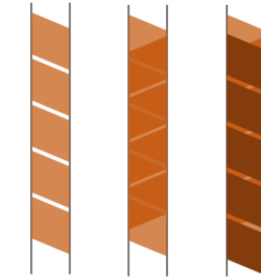
Winding on the tube

Configuration 2



1st layer 2nd layers 3rd layers

Configuration 3



1st layer 2nd layers 3rd layers

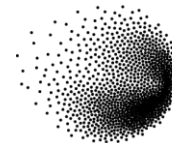
Conclusions

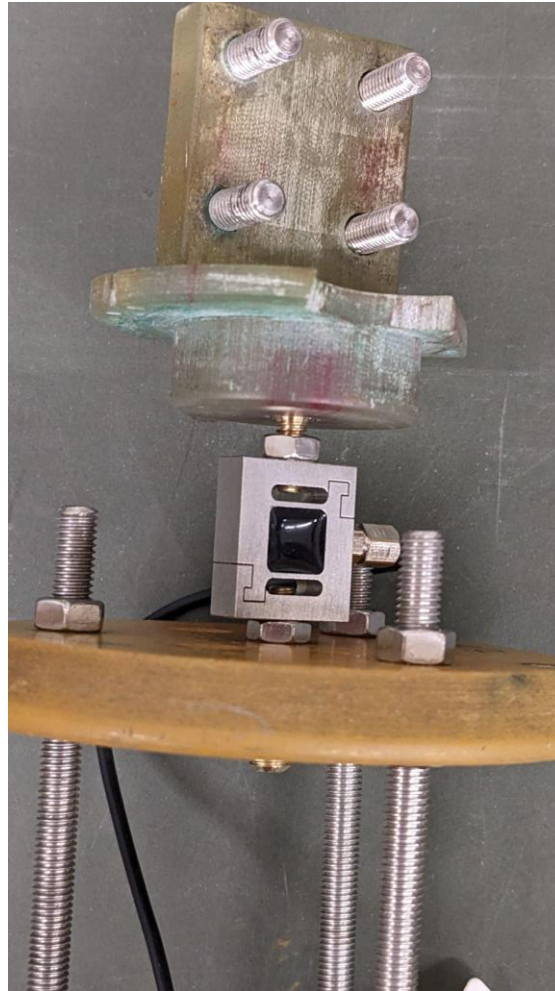
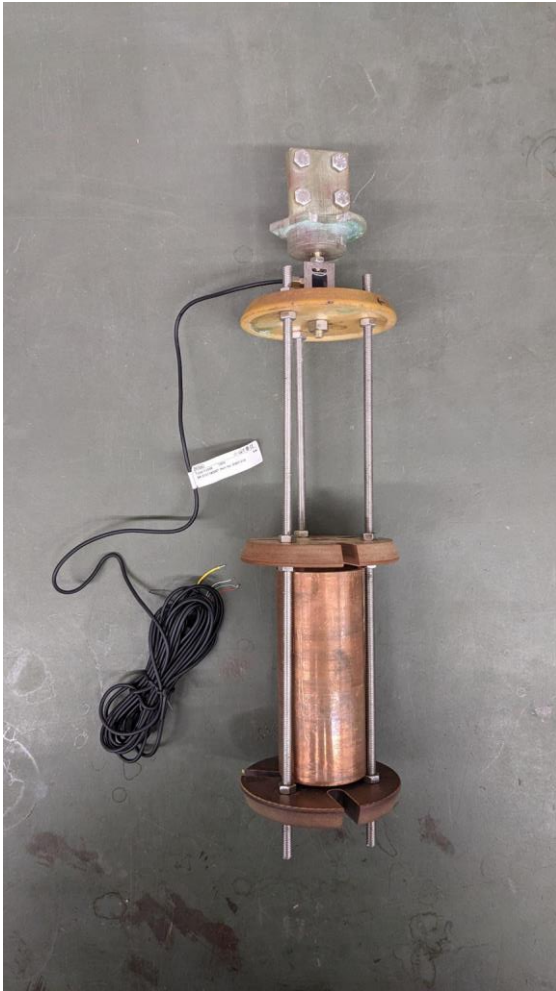
Using COMSOL Multiphysics thermal simulations designed injection channel holders with sufficient cooling power and thermal properties to reach subcritical temperature for the superconducting injection channels.

Using COMSOL Multiphysics verified that magnetic field transversal components remain under 100 mT for the particle path along the injection channels.

Measured the magnetic field shielding and forces of BSCCO2223 and NbTi hollow tubes at 4.2K.

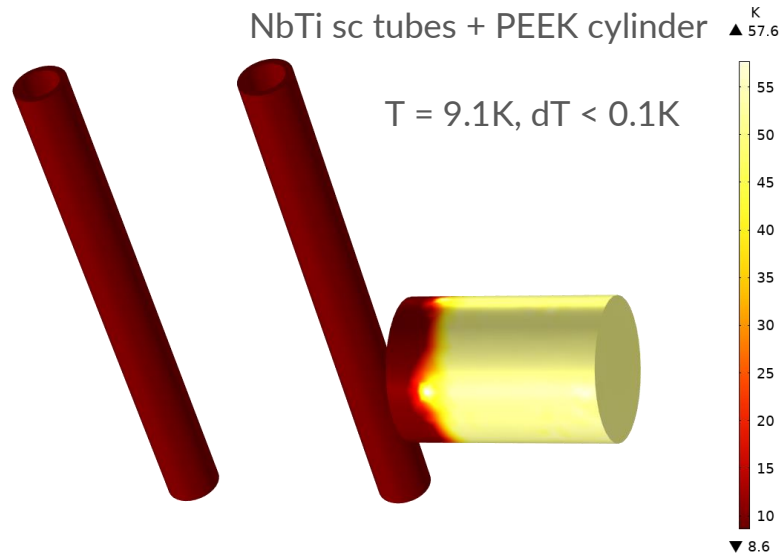
Next step is to design and investigate magnetic field shields using layered NbTi/Ti/Cu sheets, HTS tapes and combinations of different materials.



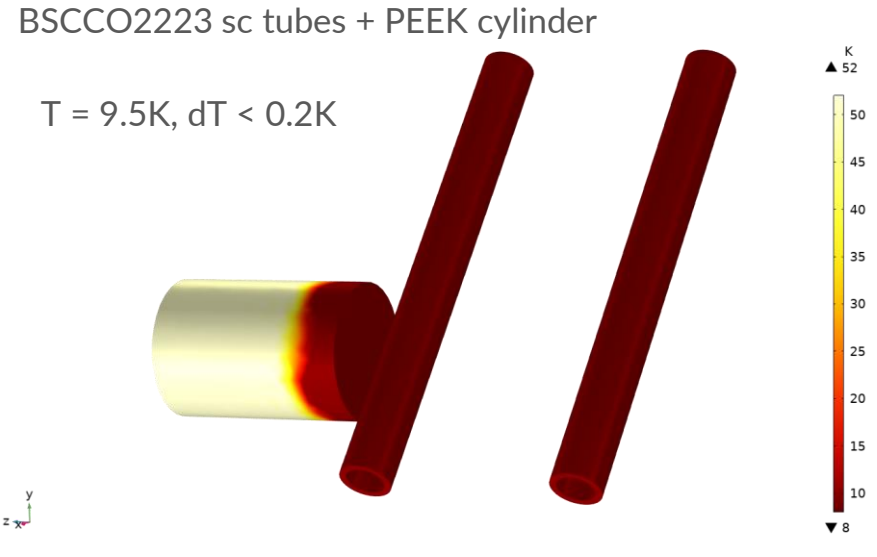


Magnetic field shielding and force measurement

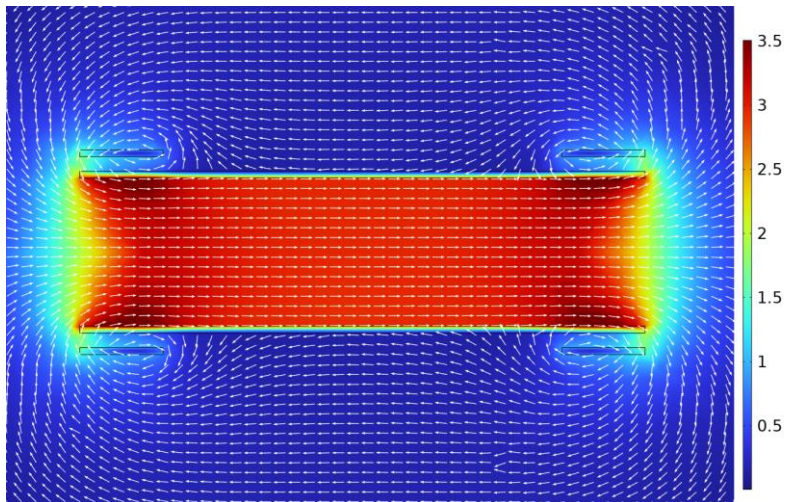
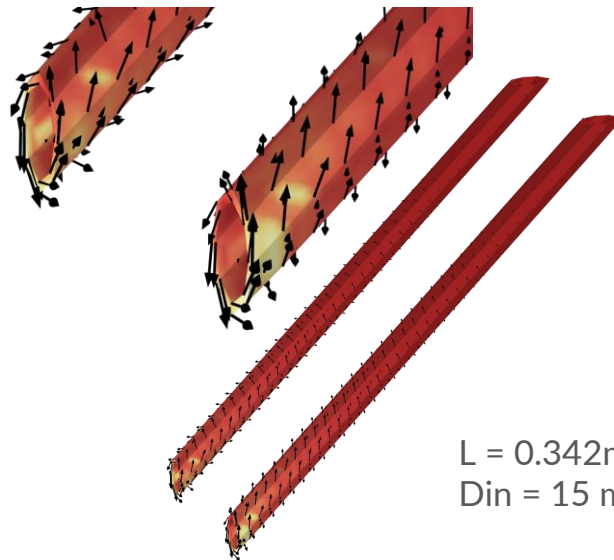
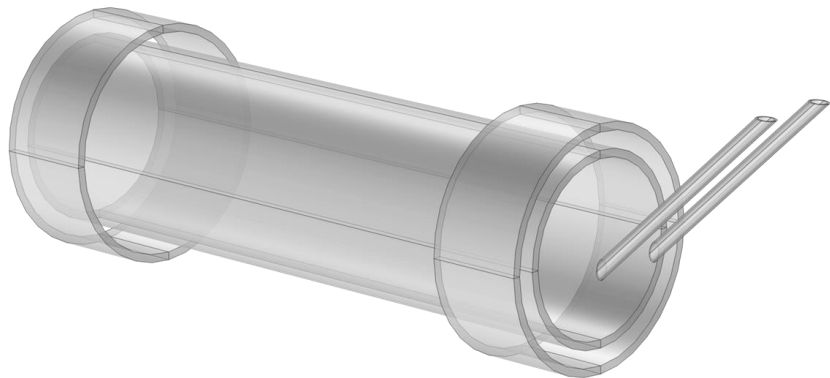
- FS28082210068-100N force sensor
- Max load 100N
- Sensitivity 2N
- According to simulations at $B = 250 \text{ mT}$ expected $F = 46\text{N}$
- Hall sensors and force sensor were calibrated at LN



Thermal simulation of the superconducting injection tubes. We assumed 8W cooling power and used PEEK cylinder in the sc tube holder with Nb-47Ti tubes. We assumed an isotropic thermal conductivity of $k = 25 \text{ W/(m K)}$ at 10K.

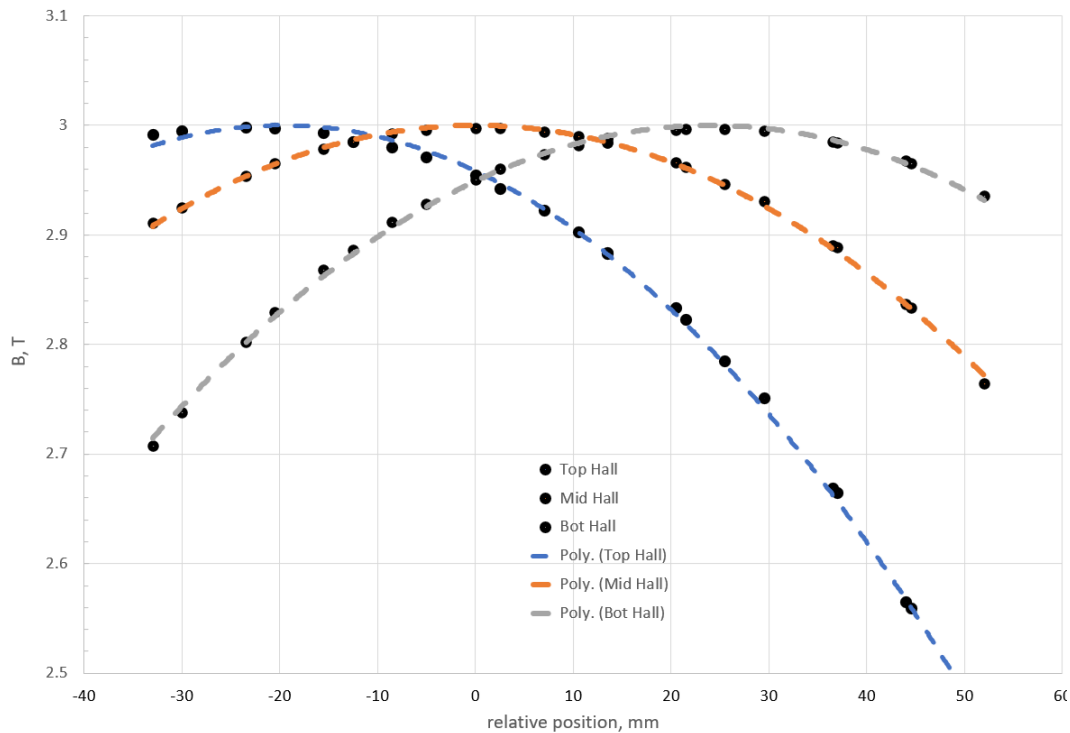


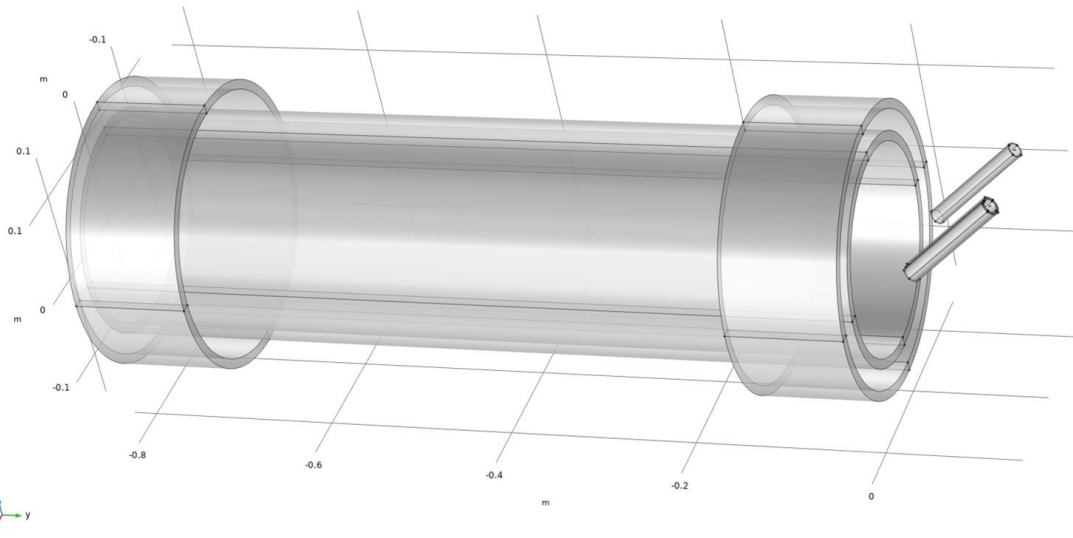
Thermal simulation of the superconducting injection tubes. We assumed 8W cooling power and used PEEK cylinder in the sc tube holder with BSCCO2223 tubes. Thermal conductivity is anisotropic $k = \{4, 4, 10\} \text{ W/(m K)}$ at 10K.



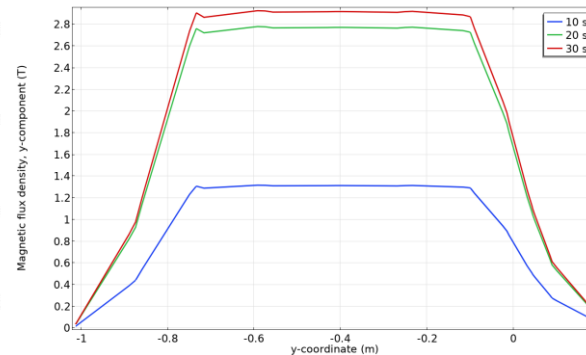
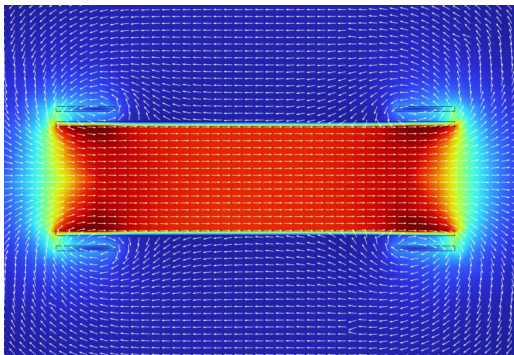
Simulated superconducting tubes. The colormap shows the J/J_C , which is the ratio of current density and critical current density at $T = 4.2\text{K}$ and $B = 3\text{T}$. The vector maps shows the flow of induced current in the superconductor.

✓ Calibrated Hall sensors + ✓ Force and magnetic field shielding measurement design





- The main coil:
 - $L = 825.5$ mm length
 - $D = 256.0$ mm with 10 mm thickness
- The shim coil $D = 298.8$ mm with 10 mm thickness
 - $L = 121.6$ mm
 - $D = 256.0$ mm with 10 mm thickness
- We use Niobium-Titanium superconducting tube
 - $L = 125$ mm
 - $D = 16.5$ mm with 1mm thickness

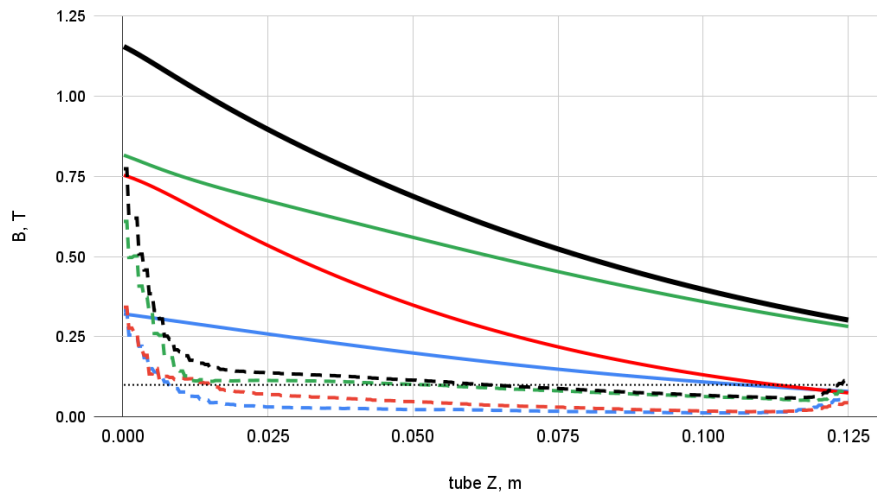


- Used A-H field formulation for the EM model
- EM model is fully coupled to thermal model
- The properties of the superconducting materials are described by $J_c(T, B)$
- Simulation run time is 27-42 minutes on 3.4 GHz

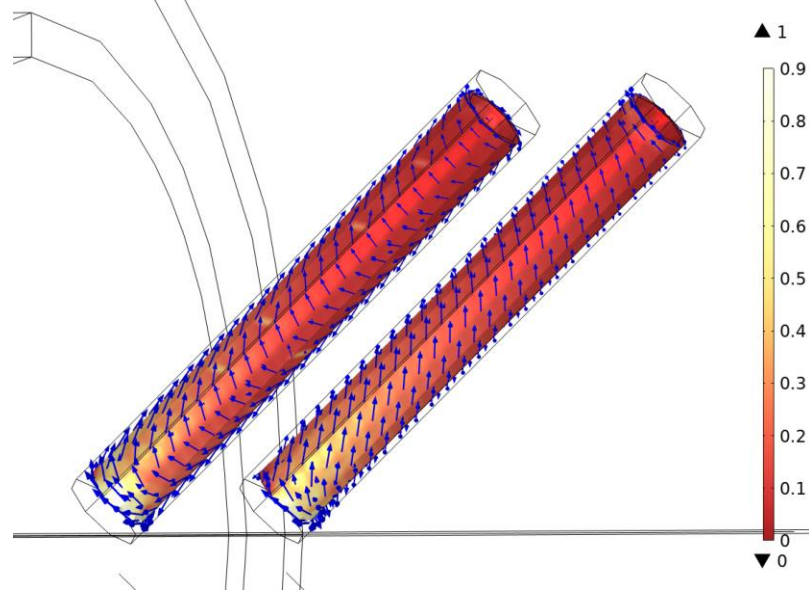
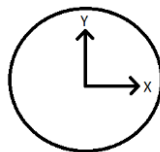
Quad-Core Intel Core i5

Magnetic field screening in superconducting NbTi tubes

- We require magnetic field in transversal direction $B < 100\text{mT}$
- B field along the axis of the sc tube can remain higher
- Color scheme illustrates the ratio of the critical current density and local current density the J/J_c



- external Bx
- external By
- external Bz
- external B
- - shielded Bx
- - shielded By
- - shielded Bz
- - shielded B
- ⋯ 100 mT



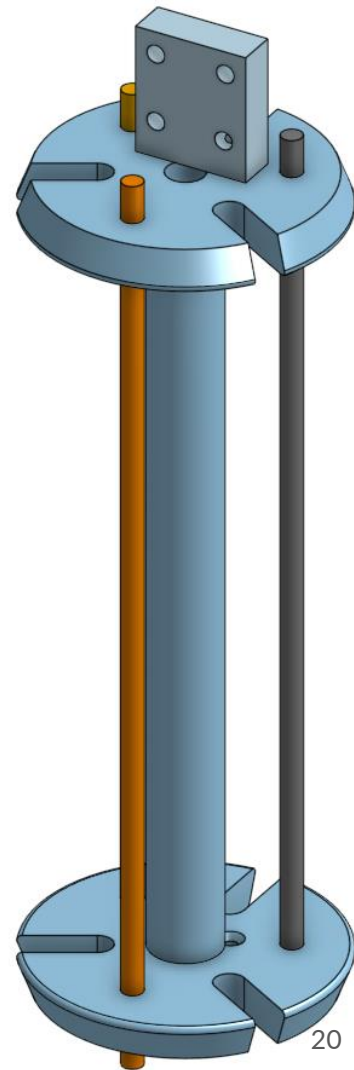
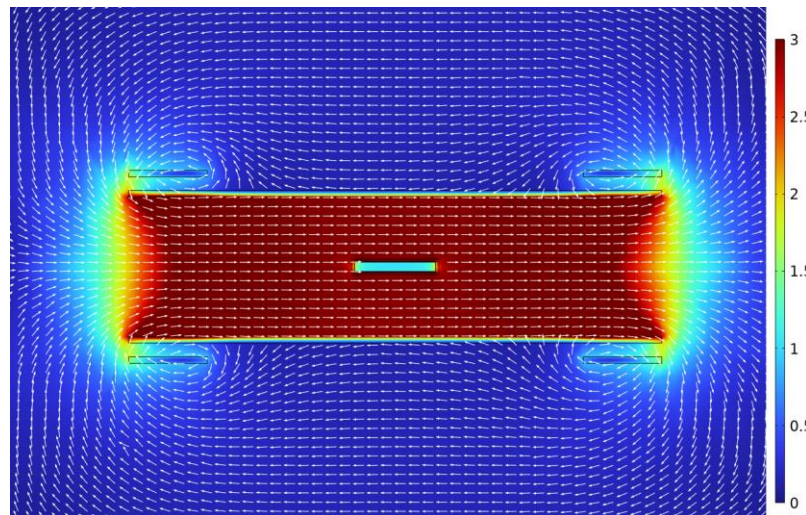
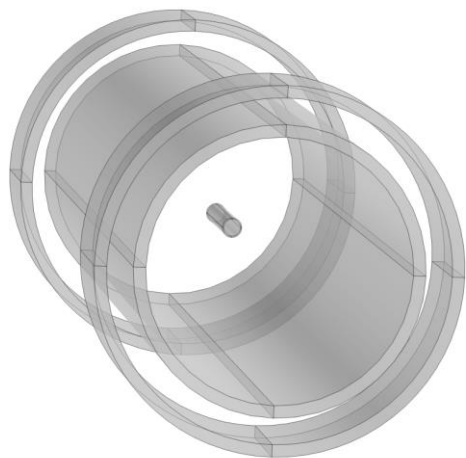
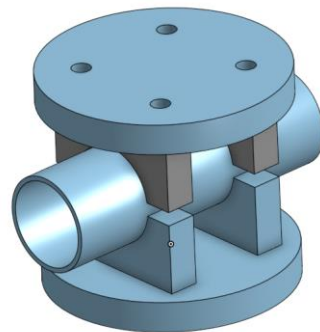
✓ B_x and $B_y < 100\text{mT}$

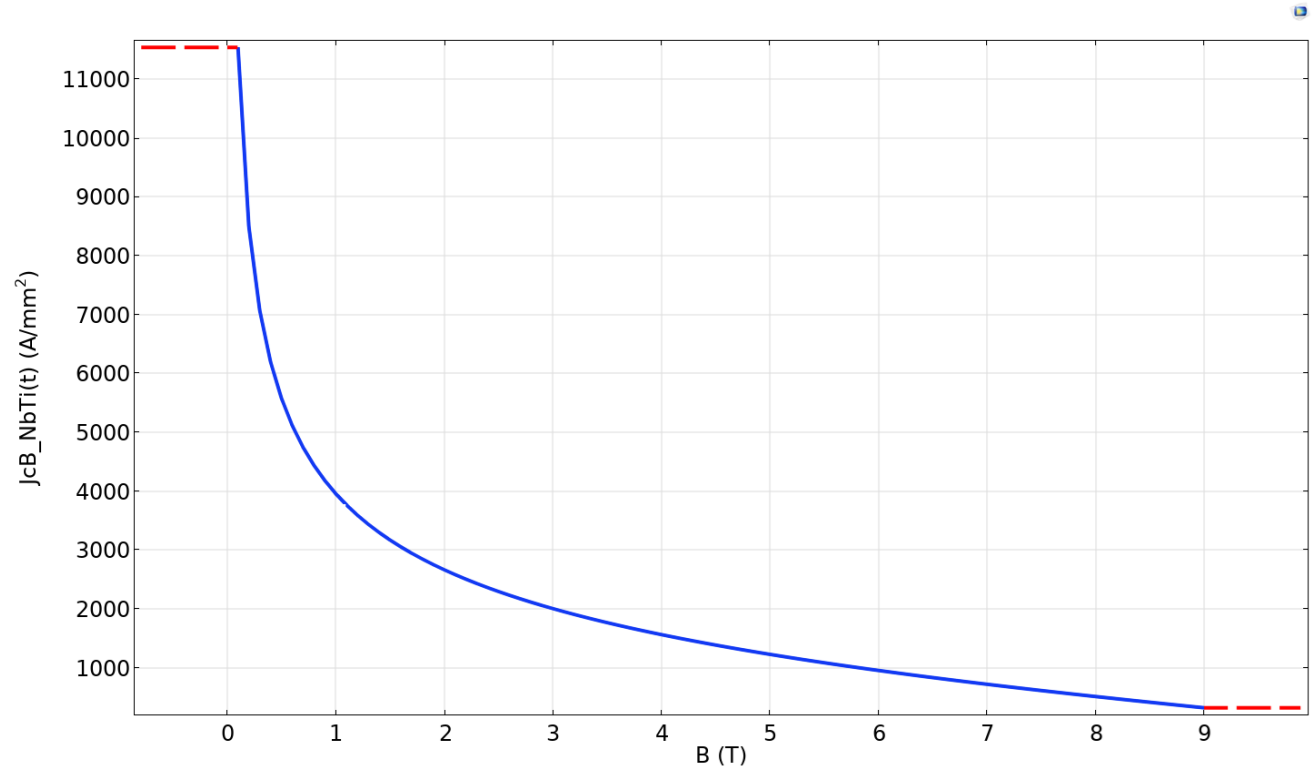
✓ $B_z \approx 100\text{mT}$

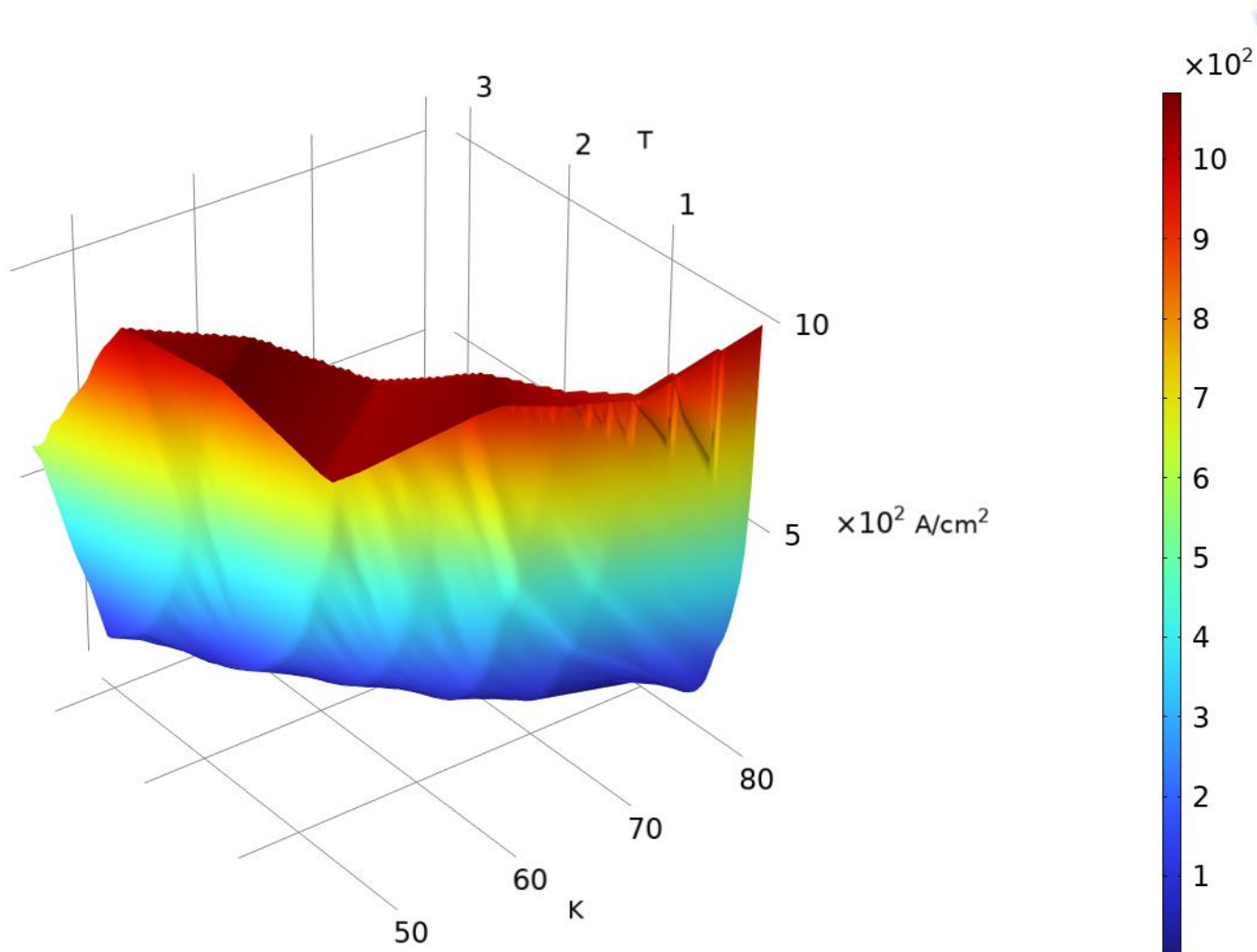
✓ Consistent shielding throughout the tube length

Measuring preparations for late July

- Measure the magnetic field screening in BSCCO and NbTi tubes in LHe
- Using 15T magnet here at **PSI**
- Planning to measure with the tube placed \parallel and \perp to **B**







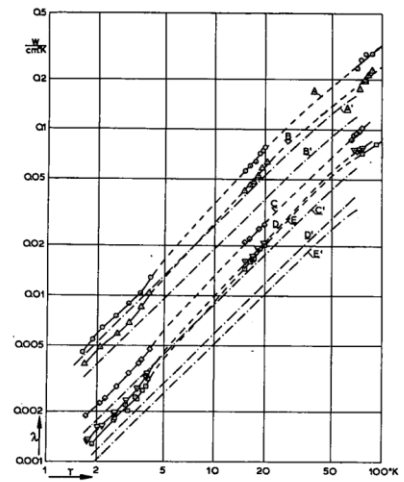
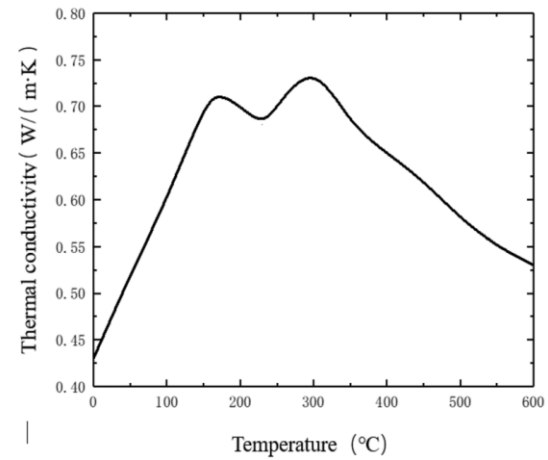
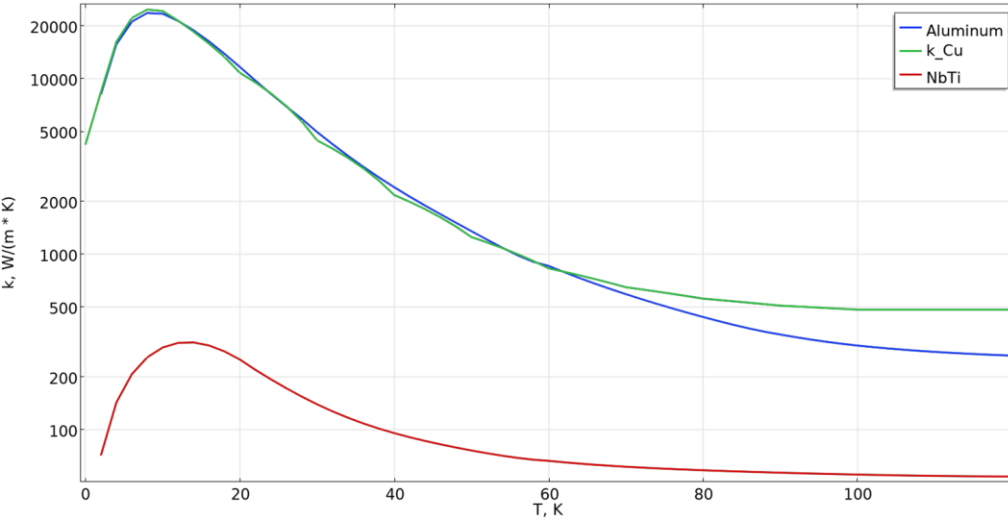
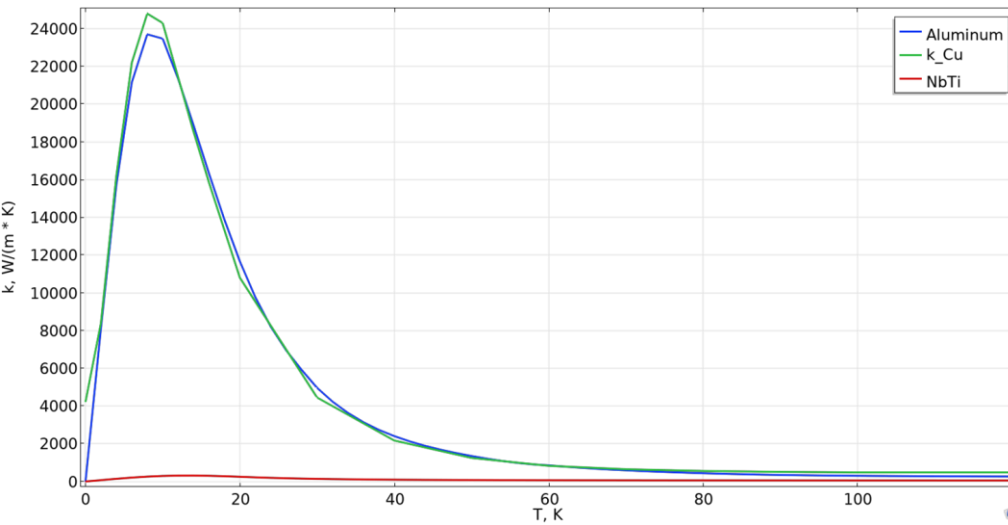


Fig. 1. The thermal conductivity λ and its electronic part λ_e of steels, both in watt/cm-deg, versus temperature in °K.

- 1287 D (curve A), △ 3703 (curve B),
- ◇ 1287 I (curve C), ▽ 1798 H (curve D),
- 3754 (curve E).

Zhao, Fuhai & Liu, Zhiqiang & Chen, Rifan & Hao, Yi & Ma, Zhihao. (2022). The effect of temperature field on the characteristics of carbon fiber reinforced thermoplastic composites in the laying and shaping process. The International Journal of Advanced Manufacturing Technology. 121. 10.1007/s00170-022-09795-9.

M.S.R. Chari, J. De Nobel, Thermal conductivity of some steels at low temperatures, Physica, Volume 25, Issues 1-6, 1959, Pages 73-83, ISSN 0031-8914, [https://doi.org/10.1016/S0031-8914\(59\)91409-0](https://doi.org/10.1016/S0031-8914(59)91409-0), (<https://www.sciencedirect.com/science/article/pii/S0031891459914090>) Abstract: Synopsis The measurements made in the Kamerlingh Onnes Laboratory on the thermal conductivity of steels at low temperatures were extended to liquid helium temperatures and the technique was improved. Five specimen of different composition and heat treatment have been investigated. The lattice conductivity is approximately proportional to $T^{1.2}$. With increasing nickel content from 2% to 27% (Ni + Cr) it decreases by about 60, 58 and 37% at the temperatures 70, 20 and 4k respectively. The electronic thermal conductivity decreases by about 80% for the mentioned temperatures.